Doctoral Forum on Vacuum Electronics (FVE 2017)

22–23 August 2017

Oversized coaxial output cavity for Ka band relativistic klystron

Shifeng Li[1,2], Zhaoyun Duan[1], Hua Huang[2], Fei Wang[1], Xin Wang[1], Zhenbang Liu[2], Hu He[2], Zhanliang Wang[1], Yubin Gong[1]

[1]*National Key Laboratory of Science and Technology on Vacuum Electronics in Chengdu, School of Physical Electronics, University of Electronic Science and Technology of China, Chengdu, People's Republic of China*
[2]*Science and Technology on High Power Microwave Laboratory, Institute of Applied Electronics, China Academy of Engineering Physics, Mianyang, People's Republic of China*
E-mail: zhyduan@uestc.edu.cn

Published in *The Journal of Engineering*; Received on 8th February 2018; Accepted on 28th February 2018

Abstract: In this study, an oversized coaxial output cavity is proposed for a Ka band relativistic klystron amplifier (RKA). It consists of a three-gap resonator and a coupler. To ensure the concentricity, the double-row supporting rods are used in the output cavity. The parameters of the output cavity are obtained through theoretical analysis and CST simulation. In addition, the authors evaluate the performance of the output cavity by using particle-in-cell software CHIPIC. They investigate the influences of the period length and the external quality factor on the output power. Furthermore, they study the effect of the overmoded ratio on power and electronic efficiency. The simulation shows that the output power reaches 1.08 GW and electronic efficiency is 36.0%. The simulated results indicate that the proposed output cavity can be used in the RKA with GW-level power at the Ka band.

1 Introduction

Recently, millimetre and sub-millimetre wave science and technology have attracted great attention, especially millimetre and sub-millimetre wave sources [1–5]. As one of the most promising devices for developing high-power microwave sources, the relativistic klystron amplifier (RKA) has attracted worldwide attention due to its unique characteristics such as high power, high efficiency, amplitude and phase stability [6–8]. However, the output power of the RKA will decrease significantly in the millimetre wave regime, which is mainly due to its physical restrictions such as the space charge limited current and the surface field breakdown [9]. Friedman *et al.* proposed an X band triaxial klystron amplifier (TKA) with a large electron beam diameter for propagating high-electron beam power and enhancing the power capacity [10]. Based on the TKA structure, simulation and experiments have been conducted to realise a GW-level microwave output at the X band [11–15]. However, a GW-level RKA at the Ka band has not been reported because the serious surface electric field breakdown and low electronic efficiency.

We combine the advantages of the TKA, overmoded structure and extended interaction technology to develop an oversized coaxial extended interaction output cavity with high-power capacity and high-electronic efficiency. The overmoded ratio of the output cavity reaches 7 (D refers to the coaxial drift tube diameter and λ refers to the operating wavelength), i.e. $D/\lambda \approx 7$. Then, we analyse the relationship between the structural parameters of the output cavity and its performance including the output power and surface electric field. Furthermore, we investigate the effect of the overmoded ratio on the power capacity, electronic efficiency and so on. In addition, we analyse the effect of double-row supporting rods on the output cavity.

2 Analysis of the oversized coaxial output cavity

The schematic of the Y–Z section of the oversized coaxial output cavity is presented in Fig. 1. It is shown that the output cavity consists of a three-gap resonator, a radial coupler, a coaxial waveguide and double-row supporting rods. In the three-gap resonator, the operation mode is TM_{01} mode, which includes the TM_{01}-π mode, the TM_{01}-π/2 mode and the TM_{01}-2π mode. According to the transit time theory, the electron beam can interact with the TM_{01} mode while passing through the output cavity. The beam–wave interaction is different for different modes. For the TM_{01}-π mode, the relationship between the power obtained by the electron beam from the high-frequency field and the direct current (DC) transit angle during the beam–wave interaction is [16]

$$P_e = \frac{I_0 U_m^2}{4U_0} F(\theta_d), \tag{1}$$

where U_m is the amplitude of the high-frequency voltage of the three-gap output cavity, U_0 is the electron beam voltage, I_0 is the electron beam current, θ_d is the DC transit angle of the gap in the output cavity and $F(\theta_d)$ is defined as [16]

$$F(\theta_d) = \frac{10 - 16\cos\theta_d + 8\cos 2\theta_d - 2\cos 3\theta_d}{\theta_d^2} - \frac{8\theta_d \sin\theta_d - 8\theta_d \sin 2\theta_d + 3\theta_d \sin 3\theta_d}{\theta_d^2}. \tag{2}$$

From (2), we can obtain the relationship between $F(\theta_d)$ and θ_d, as shown in Fig. 2. It can be seen that there is an optimal DC transit angle (where $\theta_d = 2.08$ rad) to maximise the electronic efficiency of the beam–wave interaction. Here, the electron beam voltage, electron beam current and operating frequency are set as 500 kV, 6 kA and 30.5 GHz, respectively. Thus, the propagation constant β_e of the electron beam is calculated to be 740.3 rad/m. In addition, the distance between gaps can be calculated as

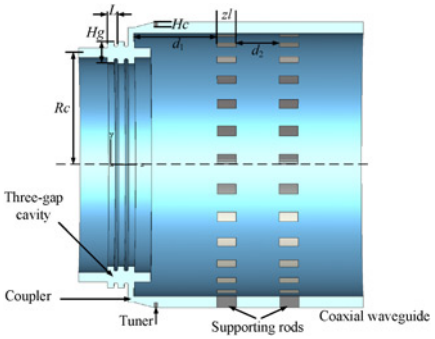

Fig. 1 *Y–Z section of schematic of the output cavity*

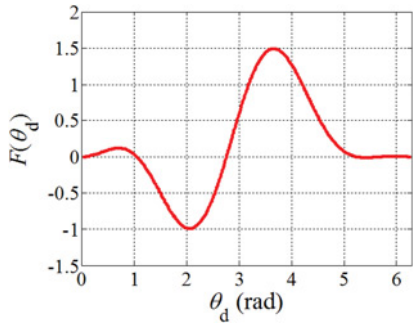

Fig. 2 *$F(\theta_d)$ versus θ_d of the three-gap output cavity*

$L = \theta_d/\beta_e = 2.8$ mm. However, considering the wall thickness between the gaps, the actual length should be >2.8 mm.

Then, we use simulation software CST [17] to investigate the resonant characteristics and mode distribution of the output cavity. In the CST simulation, we establish a model of the output cavity for simulation and optimisation, where R_c is 35 mm, L is 3.2 mm and gap width is 2.0 mm. Fig. 3 shows the group delay curve at the output port, which indicates two resonant frequencies (28.75 and 30.5 GHz). In addition, the group delay time (τ_g) is about 1.6 ns at 30.5 GHz as shown in Fig. 3. The external quality factor Q_{ext} can be calculated as $2\pi f\tau_g/4 = 86$ at 30.5 GHz [18]. Fig. 4 presents the electric field distribution at 30.5 GHz, in which the direction is opposite at the adjacent gap, that is, the mode is a π mode.

The inner and outer conductors of the output cavity are assembled and fixed by double-row supporting rods. The supporting rods are made up of N fan-shaped metal rods and $N > \pi(a+b)/\lambda$ where a and b are the inner and outer radii of the coaxial waveguide, respectively and λ is the operating wavelength [19]. In this study, $a = 41.06$ and $b = 44.56$ mm, then $N > 27.2$. Thus, we select the N as 28. For the double-row supporting rods, the distance between double-row supporting rods $d_2 = m\lambda/2$, where we set m as 2. The single-row supporting rods and double-row supporting rods are simulated and optimised by using CST. We obtain the S_{21} parameters of the supporting rods with the zl of 7.85 mm, d_2 of 9.9 mm and the angle of 2.5° as illustrated in Fig. 5, which shows that the transmission coefficient of the supporting rods is >99.7% over the 1 GHz frequency range. Figs. 6*a* and *b* present the electric field distributions with single-row supporting rods and double-row supporting rods in a coaxial waveguide, respectively. The double-row supporting rods are used in the output cavity and we can find that there is no change in the resonant frequency as presented in Fig. 7 compared with Fig. 3.

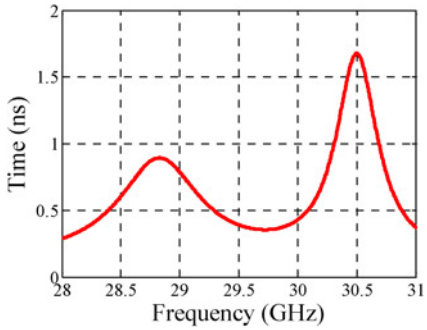

Fig. 3 *Group delay curve at the output port*

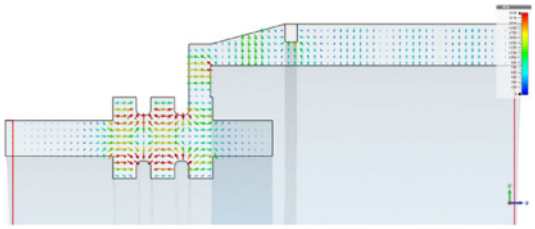

Fig. 4 *Electric field distribution at 30.5 GHz in the output cavity*

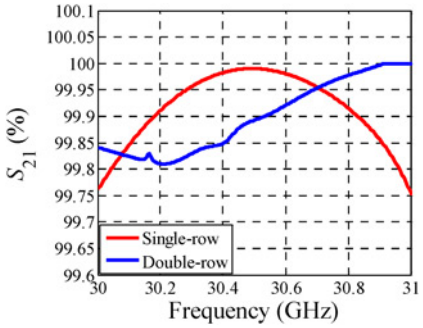

Fig. 5 *S_{21} parameters of the single row and double-row supporting rods*

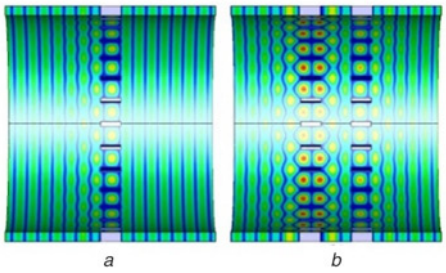

Fig. 6 *Electric field distribution at 30.5 GHz in the coaxial waveguide with supporting rods*
a With single-row supporting rods and
b With double-row supporting rods

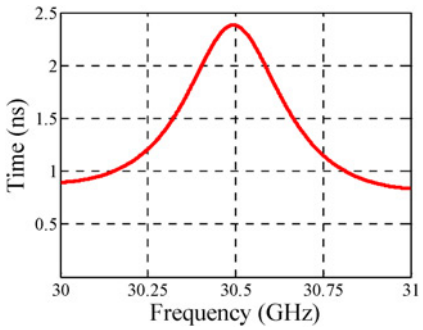

Fig. 7 *Group delay curve at output port with double-row supporting rods*

3 Simulation results and discussion

Particle in cell (PIC) simulation software CHIPIC [20] is used to simulate and optimise the structural parameters. In the PIC simulation, the beam voltage is 500 kV, the beam current is 6 kA, the axial focusing magnetic field is 1 T, the operating frequency is 30.5 GHz and the fundamental modulation depth (the ratio of the amplitude of the first harmonic to the DC) is 110%. When the pre-modulated electron beam passes through the output cavity, the electron beam energy is converted to the radio frequency (RF) field energy, and then the RF field energy is coupled to the output waveguide through the coupler. The 2.5-dimensional PIC (2.5D-PIC) simulation is used to optimise the cavity structural parameters. Two structural parameters are mainly considered: one is the period length (L) and another one is the height of the tuner (H_c). The relationship between the output power and period length is shown in Fig. 8, which indicates the optimal period length is 3.2 mm for the height of tuner (H_c) of 1.5 mm. With the period length of 3.2 mm, the external quality factor Q_{ext} of the output cavity is simulated by changing the height of the tuner (H_c), as illustrated in Fig. 9. We can find that the best height of the tuner is 1.7 mm, for which Q_{ext} is 86.

For the coaxial RKA, the operating frequency of the output cavity is only determined by the gap height (H_g), regardless of the radius of the electron beam (R_c). For the previous optimised output cavity, we only change the centre radius of the electron beam to investigate the effects of a larger overmoded ratio. As the electron beam radius increases, we study the relationship between the maximum electric field in the output cavity and different electron beam radii under the same output power of 1 GW, and the results are illustrated in Fig. 10. Fig. 10 illustrates that increasing the electron beam radius effectively reduces the electric field strength in the output cavity. Zhang *et al.* found that the breakdown threshold can reach 2.5 MV/cm by treating the slow wave structure surface [21]. The electric field intensity is lower than the breakdown threshold which means that it can be tolerated. In addition, for the diffident conditions, a suitable electron beam radius can be selected for the oversized coaxial relativistic klystron amplifier (OC-RKA).

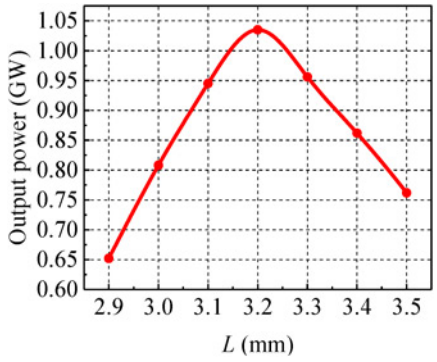

Fig. 8 *Output power as a function of period length (L)*

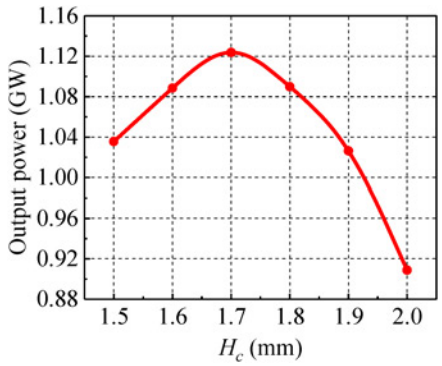

Fig. 9 *Output power as a function of height of the tuner (H_c)*

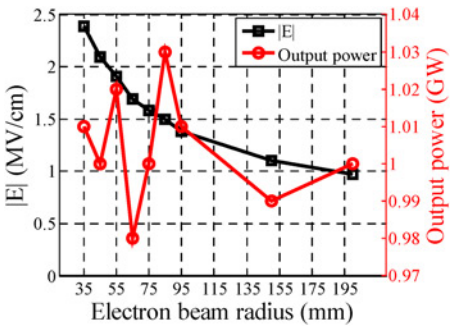

Fig. 10 *Maximum electric field and output power as a function of the electron beam radius*

In the above study, we use the 2.5D-PIC simulation method, which cannot consider the impact of the asymmetric mode. We need to study the impact of asymmetric modes on overmoded structures with the R_c of 35 mm by 3D-PIC simulation. In simulation, we model the same pre-modulated electron beam. As a result, Figs. 11*a*–*c* show the performance of the output cavity. Fig. 11*a*

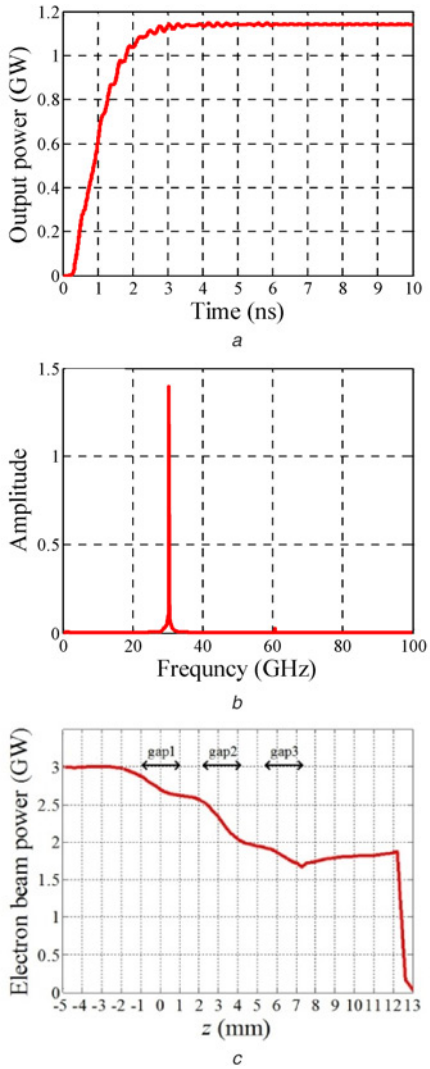

Fig. 11 *Performance of the output cavity without supporting rods*
a Output power of the output cavity without supporting rods
b Spectrum of the output signal
c Electron beam power versus axial position (z)

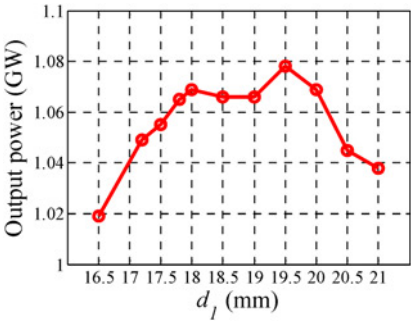

Fig. 12 *Output power versus d_1*

is the average power versus operating time for the output cavity, which demonstrates that the output cavity can generate 1.13 GW output power corresponding to the electronic efficiency of 37.6%. It is shown in Fig. 11*b* that the spectrum of the output signal is pure, which hints that there is no oscillation from the asymmetric mode such as TE_{11}, TE_{21} and so on. Fig. 11*c* presents that the electron beam power in the output cavity changes with the axial position. The primary beam–wave interaction occurs in the first two gaps with ~1 GW of electron beam power lost. The efficiency of the beam–wave interaction decreases in the third gap due to the coupling structure. However, the overall efficiency of the beam–wave interaction is high for the output cavity with 37.6%.

Since the output cavity includes a double-row supporting rods to fix the inner and outer conductors of the output cavity, we need to consider the effect of the supporting rods for the beam–wave interaction efficiency in 3D-PIC simulation. The distance (d_1) between the supporting rods and the output cavity affects the wave–beam interaction efficiency. For different d_1, we can obtain the output power as illustrated in Fig. 12, which indicates the optimal d_1 is about 19.5 mm with the output power of 1.08 GW (where $d_1 \approx 2\lambda$). It demonstrates that the supporting rods have almost no effect on the output cavity performance.

4 Conclusion

In this study, an output cavity is designed and optimised for the Ka-band oversized RKA. The resonant characteristics and mode distribution in the output cavity are studied by using CST, in which the operating mode is π-mode and the resonant frequency is 30.5 GHz. We have studied in detail the influence of structural parameters of the output cavity on the output power and the influence of the electron beam radius on the maximum electric field intensity in the output cavity. The output cavity is optimised by using CHIPIC. The output power and the electronic efficiency of the output cavity can reach 1.13 GW and 37.6%, respectively. In addition, the output cavity with double-row supporting rods is simulated. The results show that the output power is 1.08 GW and the electronic efficiency is 36.0%, which show that supporting rods have a little effect on the output cavity. The proposed output cavity has wide applications in Ka band gigawatt-level klystron amplifiers.

5 Acknowledgments

This work was in part supported by the National Natural Science Foundation of China (grant nos. 61471091, 61611130067, 61531010 and 11475158). We are grateful to Assistant Prof. Junpu Ling at the College of Advanced Interdisciplinary Studies of the National University of Defense Technology for valuable discussions and suggestions.

6 References

[1] Sirtori C.: 'Applied physics: bridge for the terahertz gap', *Nature*, 2002, **417**, pp. 132–133
[2] Sherwin M.: 'Applied physics: terahertz power', *Nature*, 2002, **420**, pp. 131–133
[3] Li S.F., Duan Z.Y., Wang F., *ET AL.*: 'Simulation study of aW-band broadband extended interaction klystron'. IVEC, Monterey, USA, April 2016, pp. 1–2
[4] Li S.F., Duan Z.Y., Wang F., *ET AL.*: 'Optimization of multigap extended output cavity for a G-band sheet beam extended interaction klystron'. IRMMW-THz, Tucson, USA, September 2014, pp. 1–2
[5] Song L.L., He J.T., Ling J.P.: 'A novel Ka-band coaxial transit-time oscillator with a four-gap buncher', *Phys. Plasmas*, 2015, **22**, (05), p. 053107
[6] Lau Y.Y., Friedman M., Krall J., *ET AL.*: 'Relativistic klystron amplifiers driven by modulated intense relativistic electron beams', *IEEE Trans. Plasma Sci.*, 1990, **18**, (3), pp. 553–569
[7] Wu Y., Xie H.Q., Li Z.H., *ET AL.*: 'Gigawatt peak power generation in a relativistic klystron amplifier driven by 1 kW seed-power', *Phys. Plasmas*, 2013, **20**, (11), p. 113102
[8] Zhao Y.C., Li S.F., Huang Z., *ET AL.*: 'Analysis and simulation of a multigap sheet beam extended interaction relativistic klystron amplifier', *IEEE Trans. Plasma Sci.*, 2015, **43**, (6), pp. 1862–1870
[9] Friedman M., Pasour J., Smithe D.: 'Modulating electron beams for an X band relativistic klystron amplifier', *Appl. Phys. Lett.*, 1997, **71**, (25), pp. 3724–3726
[10] Friedman M., Serlin V.: 'Generation of a large diameter intense relativistic electron beam for the triaxial relativistic klystron amplifier', *Rev. Sci. Instrum.*, 1990, **66**, (6), pp. 3488–3493
[11] Qi Z.M., Zhang J., Zhang Q., *ET AL.*: 'Design and experimental demonstration of a long-pulse, X-band triaxial klystron amplifier with an asymmetric input cavity', *IEEE Electron Device Lett.*, 2016, **37**, (6), pp. 782–784
[12] Ju J., Zhang J., Qi Z., *ET AL.*: 'Towards coherent combining of X-band high power microwaves: phase-locked long pulse radiations by a relativistic triaxial klystron amplifier', *Sci. Rep.*, 2016, **6**, p. 30657
[13] Liu Z.B., Huang H., Jin X., *ET AL.*: 'High power operation of an X-band coaxial multi-beam relativistic klystron amplifier', *Phys. Plasmas*, 2013, **20**, (11), p. 113101
[14] Liu Z.B., Huang H., Jin X., *ET AL.*: 'Experimental study on a long pulse X-band coaxial multi-beam', *Acta Phys. Sin.*, 2015, **64**, (1), pp. 105–113
[15] Liu Z.B., Huang H., Lei L.R., *ET AL.*: 'Investigation of an X-band gigawatt long pulse multi-beam relativistic klystron amplifier', *Phys. Plasmas*, 2015, **22**, (9), p. 093105
[16] Fan Z.K.: 'Theory analysis and experiment of the transit time tube oscillator'. PhD thesis, Beijing: Graduate School of China Academy of Engineering Physics, 1999
[17] CST Corp.: CST MWS tutorials (online). Available at: www.cstchina.cn
[18] Ding Y.G.: 'Theory and computer simulation of high power klystron' (National Defense Industry Press, Beijing, 2008), p. 243
[19] Yuan C.W., Zhong H.H., Liu Q.X., *ET AL.*: 'Scattering characteristics of metal posts in coaxial waveguide', *High Power Laser Particle Beam*, 2005, **17**, (7), pp. 1055–1059
[20] Zhou J., Liu D., Liao C., *ET AL.*: 'CHIPIC: an efficient code for electromagnetic PIC modelling and simulation', *IEEE Trans. Plasma Sci.*, 2009, **37**, (10), pp. 2002–2011
[21] Zhang J.D., Ge X.J., Zhang J., *ET AL.*: 'Research progresses on Cherenkov and transit-time high-power microwave sources at NUDT', *Matter Radiation at Extremes*, 2016, **1**, (3), pp. 163–178